Effects of Cl^- concentration on corrosion behavior of carbon steel and super13cr steel in simulated oilfield environments

X.H. Zhao [1, 2, a], Y.X. Sheng [3], C.X. Yin[1], G.F. Li[1] and Y. Han[1]

[1]*Tubular Goods Research Institute, CNPC: State Key Laboratory of performance and Structural Safety for Petroleum Tubular Goods and Equipment Materials, Xi' an 710077, China*
[2]*School of Materials Science and Engineering, Xi' an Jiao tong University, Xi' an 710049, China*
[3]*Petrochina Jidong Oilfield Company, Tangshan 063004, China*

Abstract. In order to understand the changing tendency of the corrosion behavior of carbon steel and stainless steel with different chloride ion concentration, Electrochemical method and high temperature and high pressure immersion method combined with scanning electron microscopy were used in this paper. The results show that the corrosion potential of carbon steel is almost the same at 60ºC. While for super13Cr martensitic stainless steel, its critical pitting potential sharply decreases from -48 mV to -213 mV (vs Ag/AgCl). However, with the increase of Cl^- content at 90ºC, the corrosion potential of carbon steel is gradually reduced. While for the super13Cr, the corrosion potential reduces sharply, and when the Cl^- concentration is greater than or equal to 40g/L, the corrosion potential basically remained constant, the critical pitting potential also is not obviously changed. Carbon steel corrosion is mainly controlled by the diffusion effect. Super13Cr martensitic stainless steel displays the single capacitive reactance arc.

Keywords: corrosion resistant alloy; electrochemistry; corrosion behavior; impedance spectroscopy.

1 Introduction

The corrosion problem of casing and tubing have attracted more attention of more oil and gas fields. Especially along with the increasingly extended length of oil and gas drilling time, many oil and gas wells are working in the later period, and fluid moisture content and aggressive ions increased and complicated, corrosion failures of casing and tubing are becoming more and more serious [1-3]. Cl^- is the most common and corrosive ions in the oil field environment, the corrosion failure and perforation leakage events of tubings happened repeatedly due to the presence of Cl^-. Especially in acid environment and in the presence of Cl^- with higher concentration, corrosion failure and serious damage of stainless steel tubings can be seen everywhere [4-5]. Many research about stainless steel have been done, however, most focus on the temperature, partial pressure of CO_2 / H_2S and corrosion product film, and the results consider that with the increase of chloride concentration, the corrosion rates are becoming higher [6]. But combined with the results of corrosion online monitoring, the higher of the Cl^- concentration (above 10^5 mg/L) in service medium conditions, the corrosion rates are relatively not very higher. On the contrary, in the solution environment with relatively lower Cl^-

[a] Corresponding author : zhaoxuehui@cnpc.com.cn

concentration, the corrosion rates are relatively more higher. So the applicability between the tubing materials and service environment is considered a key question. Many reference show that Cl^- has a strong corrosive to oil pipe, but without clearly defined as the concentration range of the applicability [7-9], and little attention was paid on the corrosion resistance and variation trend of carbon steel and stainless steel material at the different Cl- concentration. Carbon steel and stainless steel material have different chemical composition and organizational structure, so the corrosion mechanism of two kinds of materials are not the same in the solution medium containing Cl- [10-12]. The present work aims at investigating the electro-chemical corrosion behavior of carbon steel and super13Cr stainless steel in acidic environment containing Cl-, and comparative analysis the corrosion property differences and change trend of two kinds of materials with the different Cl- concentrations. The results of this study have an important guiding significance to oil fields for rational selection materials and hope to serve as a lead to the choosing of tubings for the oil fields.

2 Experimental

2.1 Immersion tests

Corrosion behavior were carried out on two commercially available tubings, one was P110 and the other was super13Cr, which were denoted as 1# and 2#, respectively. The compositions of the samples are given in Table 1. It can be seen from Table 1 that Ni, Cr, Mo contents were the main differences between the two materials. The specimens for immersion test were machined as rectangle coupons with dimension of 40 mm×15 mm×3 mm. A 6 mm diameter hole at one end serves to hang the specimens from a specimen stand with a non-metallic wire inside the autoclave. The specimens were first ground successively with 200, 400, 600 and 800 grit sandpaper, cleaned with alcohol and acetone, and then dried immediately. The specimens were weighed with a precision of 0.1 mg.

The simulated solution was made of Na^+ and Cl^-. N_2 gas was bubbled for 3 h to remove oxygen before CO_2 was introduced in the autoclave. Field environmental conditions were simulated at a different Cl- concentration .The test duration was 168 h. The corrosion rates were calculated from the data obtained by the weight-loss method. After 168 h of exposure, the specimens were rinsed with distilled water and then dried. Each specimen was weighed with a precision of 0.1 mg. However, the corrosion rate is the average value for 168 h. Through weight-loss method, corrosion rates were calculated as follows:

$$V = \frac{\Delta m}{\rho s t} \times 24 \times 365 \tag{1}$$

where V is corrosion rate in mm/a, Δm is the weight loss in g, ρ is the material density in g/mm^3, s is the corrosion area in mm^2, and t is the test duration in h.

Table 1. Chemical composition of two kinds of materials used in this study (wt%)

Number	C	Si	Mn	P	S	Cr	Mo	Ni	Ti	Cu
1#	0.26	0.25	1.02	0.012	0.0026	0.62	0.017	0.032	0.008	/
2#	0.016	0.45	0.46	0.013	0.0047	12.98	2.25	5.04	/	1.37

2.2 Electrochemical measurements

The potentio dynamic polarization measurements were carried out using a 273A Electrochemical Measurement System manufactured by EG&G. The tests were carried out in a three-electrode system. The samples for electrochemical test were employed as the working electrode, the size of samples was ϕ10 mm×5 mm. The reference electrodes are silver, silver chloride electrode (Ag/AgCl) with saturated potassium chloride (KCl) solution. The auxiliary electrode was a pair of graphite poles. Working

electrodes were polished with silicon carbide papers from 400-grit to 1000-grit, degreased with acetone and rinsed with deionized water, dewatered with ethanol prior to the experiment. The test solution was deaerated by purging CO_2 (99.95%) for 2 h. Gas exit was sealed with water.

The potentio dynamic polarization curves were recorded at a constant sweep rate of 0.3 mV/s from -100 mV~800mV with respect to the open circuit potential (E_{corr} vs Ag/AgCl). According to the oil field environment, the electrochemical experiments were performed at 60°C and 90°C and the Cl^- concentration are 20 g/L, 40 g/L and 120g/L, respectively. The choice of Cl^- concentration in the test was based on the environment of the Tarim Oilfield, which can show the trend of corrosion of materials.

The electrochemical impendence spectroscopy (EIS) measurements were carried out at open circuit potential using an alternating current voltage amplitude of 5 mV. The frequency varied from 10^5 Hz to 10 mHz. Data were presented as Nyquist plots.

3 Results and discussion

3.1 Effect of Cl^- on corrosion rate and corrosion product films

Table 2 shows the corrosion rates of samples at the high temperature and high pressure with different Cl^- concentrations. The test temperature was 110°C and the CO_2 partial pressure was 4 MPa. We can see that the corrosion rates of 1# were higher than that of 2#, the corrosion rates increases firstly and then decreases with increasing Cl^- concentration from 20g/L to 120g/L. When the Cl^- concentration was 40g/L, the result appears that the corrosion rates have a peak, and reaches the maximum value. This means that certain amounts of Cl- concentration can accelerate the anodic reaction [13] and increase corrosion rates. The anodic reaction as shows (2)-(3):

$$Fe \rightarrow Fe^{2+} + 2e \tag{2}$$
$$Fe^{2+} + CO_3^{2-} \rightarrow FeCO_3$$

$$Fe + HCO_3^{2-} \rightarrow FeCO_3 + 2e + H^+ \tag{3}$$
$$Fe + CO_3^{2-} \rightarrow FeCO_3 + 2e$$

Table 2. Corrosion rates of samples in solution with different Cl^- concentration

Materials	Corrosion rates (mm/a)		
	20g/L	40g/L	120g/L
1#	2.56	3.92	3.68
2#	0.0041	0.0069	0.0092

And for the 2# sample, the corrosion rates increases with increasing Cl^- concentrations. Fig. 1 shows the SEM profiles of the corrosion product films on 2# samples, and obvious pitting corrosion phenomena were observed on the surface of 2# with increasing Cl^- concentrations. At a content of 20 g/L (Fig. 3(a)), a thin layer of corrosion product film was observed and the tiny pitting also can be found on the surface of the sample. At a content of 40 g/L (Fig. 3(b)), the pitting is small but more obvious, at a content of 120 g/L (Fig. 3(c)), the pitting is relatively bigger. As we all know that the radius of Cl^- is small, Cl^- can penetrate through the corrosion product film and aggregate on metal surface. In addition, when Cl- and other anions coexist, particularly when the content of Cl^- is higher, Cl^- is preferentially absorbed on metal surface [14]. So a high amount of Cl^- can aggregate in the link boundaries between the metal surface and corrosion product films. Therefore, the adhesion of the link boundaries decreases, making the corrosion product films easily remove from the metal surface automatically. Thus, pitting appear on the surface of samples. At this test conditions, only the Cl- concentration is a variable, and the higher Cl^- concentration can significantly reduce the CO_2 solubility and decrease the opportunities of H^+, H_2O, H_2CO_3 and HCO_3^- to participate in the reaction, so we can

conclude that Cl^- can accelerate corrosion rates within certain concentration. The main corrosion type of 1# samples was uniform corrosion.

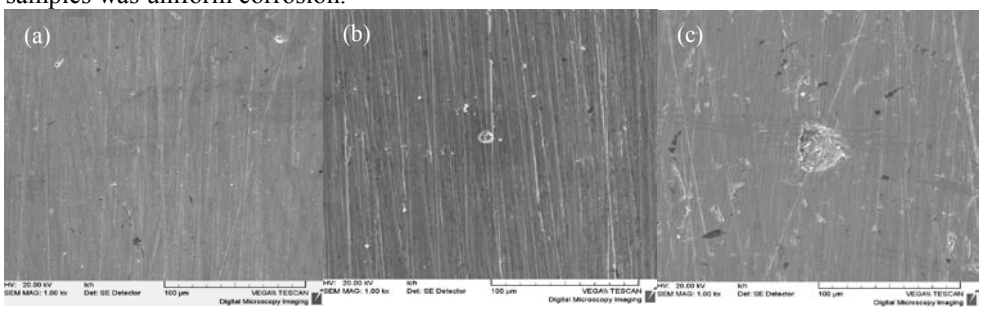

Figure 1. SEM morphology results of 2# for immersion containing different Cl^- concentration at110°C. (a) 20 g/L, (b) 40 g/L, (c) 120 g/L.

3.2 Effect of cl- concentration on electrochemical performance

Fig.2. shows the polarization curves of 1# sample at the different temperatures with various Cl- concentrations. It can be seen that the corrosion potential (Ecorr) and corrosion current density (Icorr) keep a slightly change as Cl- concentration increasing from 20 to 120 g/L at 60°C(Fig. 2a), and Ecorr was almost -700 mV. At 90°C, the Ecorr moves first to a more negative direction, and then to positive direction as Cl- concentration increasing from 20 to 120 g/L (Fig. 2b). It is obvious that increasing Cl- concentration can increase the rate of the anodic reaction. In this presence of Cl- in corrosive medium, Cl- could promote the iron dissolution through a catalytic mechanism and formed intermediate corrosion species and accelerated corrosion reaction [15-18]. So Cl- is the main reason in increasing the corrosion rate of samples. The anodic reaction process is as follows [19]:

$$Fe + Cl^- + H_2O = [FeCl(OH)]^-_{ad} + H^+ + e \tag{2}$$

$$[FeCl(OH)]^-_{ad} \rightarrow FeClOH + e \tag{3}$$

$$FeClOH + H^+ = Fe^{2+} + Cl^- + H_2O \tag{4}$$

The Fig. 2 also indicated that the corrosion properties of 1# sample was mainly affected by the test temperature. At higher temperature (90°C), the activity of material surface was strengthen from the thermodynamic point of material, and electron transferring between the solution medium and material surface were intensified, the reaction speed was improved. Meanwhile the activity of Cl- penetrate through the corrosion product film also be strengthened, therefore, the effect of Cl- on corrosion properties of materials is also affected by the test temperature.

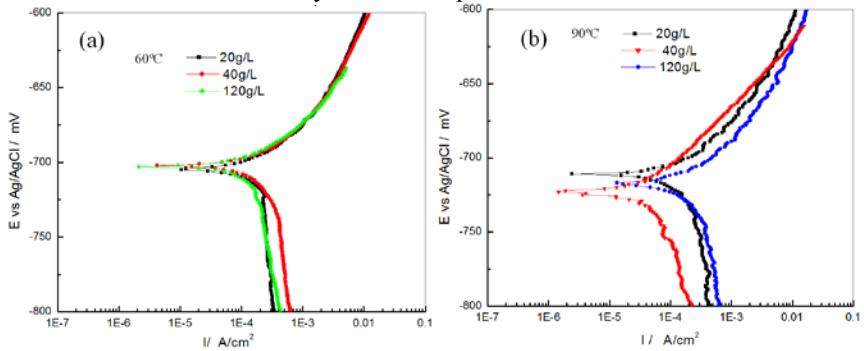

Figure 2. Potentiodynamic polarization curves of 1# tubing materials in different Cl^- containing solution at (a)

60°C and (b) 90°C.

The potentiodynamic polarization curves of 2# sample were shown in Fig. 3, and the E_{corr} and I_{corr} were obtained from the curves. It was clear that the polarization curves show a better passivation characteristic at 60°C and 90°C. At 60°C, when the concentration of Cl- was 20g/L, the E_{corr} was -499 mV. Fig. 3(a) shows that the E_{corr} first increased and then decreased as the increase of the Cl^- concentration, and the critical pitting potential (E_{pit}) of 2# appeared an obvious change. When the test temperature was 90°C, we can see from the Fig. 3(b) that the polarization curves also have an obvious passivation region, but the change trend of E_{corr} and I_{corr} are different from that of the low temperature conditions. The Fig. 3(b) shows the E_{corr} decreased with the concentration of Cl^- increased from 20g/L to 120g/L, meanwhile when the concentration of Cl^- increased from 40g/L to 120g/L, the E_{corr} changed almost no longer. This indicated that the corrosion resistance of 2# material was not affected obviously by the concentration of Cl^- when the Cl^- content increased to a value. As a result, the E_{pit} showed a similar values with the different concentration of Cl^- at the higher test temperature of 90°C. The results proved that when the concentration of Cl^- over a certain range of values, the pitting corrosion sensitivity tended to a steady value, and the pitting corrosion sensitivity of super13Cr was controlled by the test temperature. Passivation film was affected by a combined action of test temperature and Cl^-, and broken suddenly at some moment, the pitting corrosion happened.

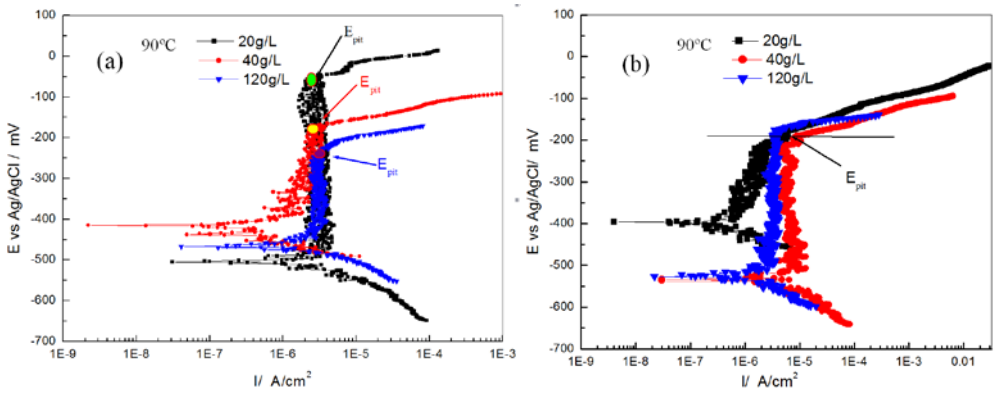

Figure 3. Potentiodynamic polarization curves of 2# tubing materials in different Cl- containing solution at (a) 60°C, (b) 90°C.

Comparative analysis the material composition and reaction mechanism, it was clear that the chemical composition of super13Cr contain relatively higher alloying elements, especially Ni, Cr, Mo elements, which have better corrosion resistance properties at high temperature and formed passivation film easily. So the compactness of corrosion scale and corrosion resistance have a close relationship with reaction temperature. Combined with the test results of the polarization curves in Figs. 2 and 3, the change trend of corrosion properties of carbon steel and super 13Cr material were shown in Fig. 4.

It can be easily seen from Fig. 4 that when the concentration of Cl- was 20g/L, the E_{pit} has a big change with the temperature increased from 60°C to 90°C, and the potential difference (ΔE_{pit}) equal to 161 mV. The result indicated that when the temperature increased, the reaction rate of the solution medium and the sample surface were accelerated, and strengthened the activity of this corrosion system. Meanwhile, the penetrating ability of erosion ion into the corrosion film also was strengthened along with the rise of temperature, and the film was breakdown at relatively low corrosion potential, the pitting failure happened suddenly.

From the Fig. 4(a), when the concentration of Cl- increased from 20g/L to 120g/L, the E_{pit} reduced from -48mV to -213 mV, and the Icorr have not obviously changed, and kept the same order of magnitude. Comparative analysis the results of the different test temperatures, it was clear that when test temperature was higher as 90°C(as Fig. 4(b)), the E_{pit} of 2# sample almost maintained around -200 mV with the increase of the Cl- concentration, but the E_{pit} gradually reduced at 60°C. This

indicated that the E_{pit} was mainly controlled by the breakdown potential of passivation film at high temperature and was mainly controlled by penetration of Cl- at low temperature. However, the combined effect of the test temperature and chloride ions increased the corrosion susceptibility leading to a lower corrosion resistance. The E_{corr} of 1 # carbon steel showed a slightly tended toward more negative values as the Cl- concentration increased (as Fig. 4(b)).

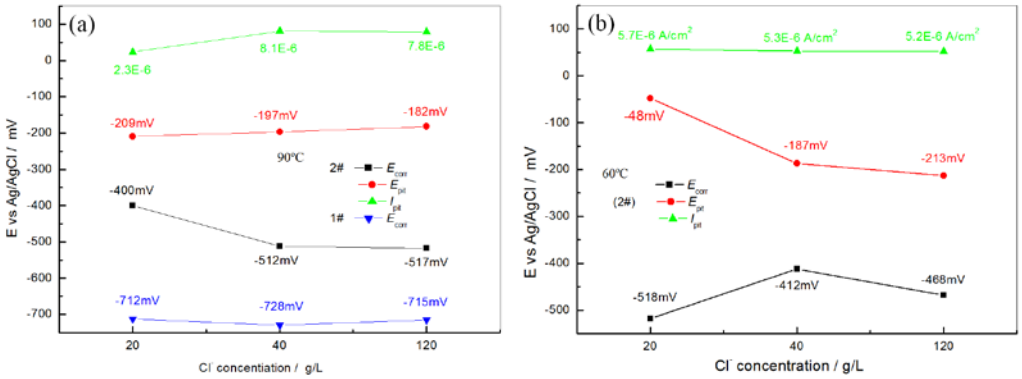

Figure 4. The changing trend of corrosion parameters of 1# and 2# in different Cl^- containing solution at (a) 90°C and (b) 60°C.

3.3 Impedance spectroscopy (EIS)

Electrochemical Impedance Spectroscopy (EIS) has been used as an interesting technique to characterize the electrochemical behavior of metal materials. However, In these cases, the most common equivalent circuit also used to describe the carbon steel tubing electrochemical behavior. Fig. 5 (a) shows the EIS of 1# sample at 90°C in different Cl- concentration. In order to keeping the samples in the same conditions before testing, the test samples were immersed in the test solution and keep 60 mins, then testing and analyzing the impedance. It was clear that the shape and size of these impedance spectra strongly depended on the Cl- content. When the concentration of Cl- was 20g/L, it shows a single impedance arc characteristics, and this indicated that the corrosion scale was dense and stable, and the Cl- adsorbing on the surface have a smaller influence on the corrosion scale. The reaction process is mainly controlled by electrochemical process. With the increase of Cl- concentration and greater than or equal to 40g/L, the impedance espectra consisted of two capacitive loops. But the high frequency capacitive loop was very small, which indicated the very severe local corrosion occurred. However, Warburg impedance was found in low frequency region as the Cl- content increased to 40g/L. It revealed that with the increase of corrosive ion concentration, the corrosion product film forming on the sample surface were not enough dense, and existed the ion diffusion channels, corrosion product film could not fully cover the surface of the sample, the electrode system was mainly controlled by the diffusion. When the Cl- concentration increased to 120g/L, the impedance spectrum characteristics changed not obvious, but the capacitive reactance arc radius in high frequency significantly less than that of 40g/L values, it shows that under the high Cl- concentration the polarization resistance of the sample reduced, the corrosion resistance decreased. Whereas, obvious departure from the beeline the Warburg impedance was. It has been explored that a capacitive loop would add on the Warburg impedance when slight local corrosion bourgeoned [20].

Fig. 5 (b) shows the impedance spectra of corrosion resistant alloy 2 # sample under the different Cl- concentrations. It indicated that the impedance spectra have the similar characteristics, and all of them show the single capacitive reactance arc with different radius, this illustrated that the corrosion film has a good capacitive resistance and has good protection for the materials. And when the Cl- concentration was greater than 20g/L, the capacitive reactance arc radius reduced obviously, this showed that when corrosive ions concentration exceeds a certain range, the corrosion resistance of 2 # material greatly reduced.

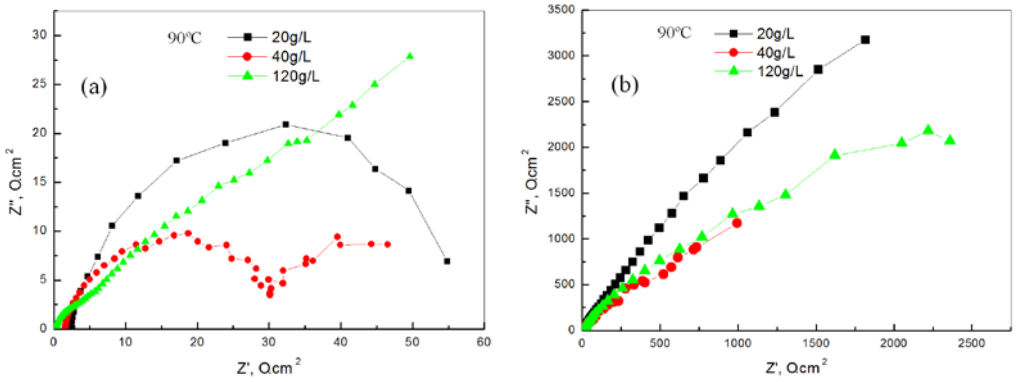

Figure 5. EIS plots of 1# , 2# materials in different Cl^- containing solution at 90°C (a) 1# and (b) 2#

So fitted the experimental results of 1# with ZSimpWin software, and got the equivalent circuit and can be expressed as the Rs (RPW) (Q). Due to the electrode frequency response characteristics of the electric double layer capacitance existed deviation with the capacitance, and phase Angle component Q instead of pure capacitance, the impedance expressions as denote equation 2 [21], and the Warburg diffusion impedance as denote equation 3 [21]. The electrode system existed dispersion effect.

$$Z_Q = \frac{1}{Y_0}(jw)^{-n} \tag{2}$$

$$Z_W = \frac{1}{Y_0}(2w)^{-\frac{1}{2}}(1-j) \tag{3}$$

The fitting results as shown in Table 3, according to the equations 2 and 3, it was clear that with the increase of Cl- concentration, impedance values are reduced. This implied that increasing Cl- concentration can speeded up the damaging process of corrosion product film, corrosion were more likely to happen. Fitting error of the EIS parameters were less than 10%.

Table 3. The fitting results of impedance spectrum under different Cl^- concentration

Concentration	R_s (ohm·cm^2)	Q(CPE)		R_p (ohm·cm^2)	Warburg Y_0(S·sec^n/cm^2)
		Y_0/ (S·sec^n/cm^2)	n		
40g/L	1.39	0.0024	0.76	27.3	0.1119
%Error	1.56	6.5	1.5	2.4	8.1
120g/L	1.30	0.0048	0.8	10.62	0.2398
%Error	3.08	7.2	3.1	6.5	6.1

Fitting results agreed well with the results of the measured impedance, as shown in Fig. 6. This explained that the equivalent circuit can reflects the actual corrosion process of 1 # carbon steel in test solution which Cl- concentration greater than 20g/L.

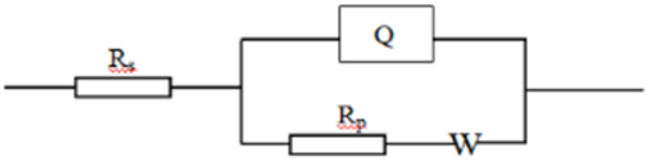

Figure 6. The equivalent circuit of the 1# material in 40,120 g/L Cl^- containing solution at 90°C

4 Conclusions

(1)At 60°C, when the Cl^- concentration increased from 20g/L to 120 g/L, the corrosion potential and corrosion current density of carbon steel changed not obviously. While for super13Cr corrosion resistant alloy, an stable passivation region were obtained, and the corrosion potential first increased and then decreased, its critical pitting potential decreased obviously and from -48 mV to -213 mV.

(2)At the higher test temperature of 90°C, the corrosion potential of carbon steel was gradually reduced with the increase of Cl- concentration, and the corrosion potential of super13Cr reduced sharply, but the critical pitting potential was not obviously changed. When the concentration of Cl^- was higher than 20g/L, the corrosion potential of super13Cr almost remain unchanged.

(3)When the concentration of Cl^- was greater than 20g/L, the impedance spectroscopy of carbon steel showed a Warburg impedance characteristics. Carbon steel corrosion was mainly controlled by the diffusion effect. Super13Cr corrosion resistant alloy displayed the single capacitive reactance arc.

(4)When the Cl^- concentration is higher than 40g/L, The pitting sensitivity of Super 13Cr was higher at 90°C, an obvious pitting phenomenon was observed.

Acknowledgement

The authors are grateful for the financial supports from the China National Petroleum Corporation for the technology project (2011D-4603-0102), and the Shaan xi Province Nature Science Foundation of China under Contracts of 2012JQ6014.

Conflicts of Interest

The authors declare no conflict of interest.

References

1. Zhu, S.D., Fu, A.Q., Yin, Z. F., *Corrosion Science*. vol. **53**, p. 3156 (2011)
2. Ren, C.Q., Liu, D.X., Bai, Z.Q., *Materials Chemistry and Physics*. vol. **93**, p. 305 (2005)
3. Li, D. G., Feng, Y. R., Bai, Z.Q., *Applied Surface Science*. vol. **253**, p. 8371 (2007)
4. Machuca, L.L., Bailey, S.I., Gubner, R., *Corrosion Science*. 2012, vol. **64**, p. 8 (2012)
5. Nesic, S., John, P., Vrhova, M., *Corrosion Reviews*., vol. **15**, p. 112 (1997)
6. Gray, L.G., *Corrosion/98*. Houston: NACE, **40** (1998)
7. Banas, J., Lelek-Borkowska, U., Mazurkiewicz, B., Solarski, W., *Electrochim Acta.* vol. **52**, p. 5704 (2007)
8. Chen, C.F., Lu, M.X., Zhao, G.X., *Journal of Chinese Society for Corrosion and Pro*. vol. **23**, p. 21 (2003)
9. Kermani, M.B., Morshed, A., *Corrosion*., vol. **8**, p. 659 (2003)
10. Moreira, R.M., Franco, C.V., *Corrosion Science.* vol. **46**, p. 2987 (2004)
11. Stephen, N.S., Michael, W.J., *Corrosion 2006*. No.06115, San Diego. 1-26 (2006)
12. MA, L.P., WANG, Y.Q., Zhao, S.H., *West-China Exploration Engineering*. vol. **11**, p. 50 (2006)
13. Liu, Q.Y., Mao, L.J., Zhou, S.W., *Corrosion science.* vol. **84**, p. 165 (2014)
14. Jiang, X., Nesic, S., Kinsella, B., Brown, B., Young, D., Corrosion. vol. **69**, p. 15 (2013)
15. Zhang, G.A., Cheng, Y.F., *Electrochimica Acta.* vol. **56**, p. 1676 (2011)
16. Marcelina, S., Pébèrea, N., Régnierb, S., *Electrochimica Acta.*, vol. **87**, p. 32 (2013)
17. Bai, Z.Q., Chen, C.F., Lu, M.X., Li, J.B., *Applied Surface Science.* vol. **252**, p. 7578 (2006)
18. Lin, C., Li, X.G., Dong, C.F., Materials. vol. **14**, p. 5 (2007)
19. Nesic, S., Thevenot, N., Crolet, J.L., Corrosion/1996, NACE, Houston, paper No.3 (1996)
20. Cao, C.N., Zhang, J.Q., An Introduction to Electrochemical Impedance Spectroscopy, Science Press: Beijing, p. 231 (2002)

